12th IEA Heat Pump Conference 2017

Study of a Massive Electricity Storage System Based on CO_2 Transcritical Heat-Pump and Power Cycle and a Geothermal Heat Transfer Process

N. Tauveron[a,*], E. Macchi[b], T. Tartière[c], D. Nguyen[d], C. Colin[b], F.-X. Lacroix[e]

a CEA, LITEN – DTBH/SBRT/LS2T, 17 rue des Martyrs Grenoble, 38054, France.
b IMFT, Université de Toulouse, 2 Allée du Professeur Camille Soula, 31400 Toulouse, France.
c Enertime, 1 rue du Moulin des Bruyères Courbevoie, 92400, France.
d BRGM Languedoc-Roussillon, 1039 rue de Pinville, 34000 Montpellier, France.
e ENGIE-CRIGEN, 361 Avenue du Président Wilson, 93210 Saint-Denis, France.

Abstract

Multi-megawatt thermo-electric energy storage based on thermodynamic cycles is a promising alternative to PSH (Pumped-Storage Hydroelectricity) and CAES (Compressed Air Energy Storage) systems. The size and cost of the heat storage are the main drawbacks of this technology but using crystalline superficial bedrock as a heat reservoir could be a readily available and cheap solution. In that context, the aim of this work is i) to assess the performance of a massive electricity storage concept based on CO_2 transcritical cycles and ground heat exchangers, and ii) to carry out the preliminary design of the whole thermal doublet system including the reservoir using ice for latent cold storage. This later includes a transcritical heat pump as the charging process (~1-10 MWe).

Various technical studies are undertaken to assess the performance of such system. Steady-state thermodynamic models have been realized to optimize system efficiency, including the investigation of regenerative or multi-stage cycles. In addition, unsteady models of geothermal heat exchanger network were developed for the ground heat storage. Coupling between different models has also been achieved. Finally an experimental device has been designed and built to test the heat-exchange dynamics with conditions are intended to reproduce real process dynamics at a laboratory scale (heat exchanger 1/10e scale ~ 1.6 m high, real temperature ~130°C and pressure conditions ~12MPa).

Keywords: ORC, CO2, electricity storage, granite

* Corresponding author. Dr. N. Tauveron
CEA, LITEN – DTBH/SBRT/LS2T, 17 rue des Martyrs Grenoble, 38054, France
nicolas.tauveron@cea.fr ; +33 438786151 (phone) ; +33 438785161 (fax)

1. Introduction

The massive integration of intermittent renewable energy production generates new challenges for the supervision and regulation of electric grids. The variability and unpredictability of these sources conflict with the reliable supply of electricity required by industries and consumers: energy storage is essential to balance supply and demand. Energy storage will also play a key role in enabling to develop a low-carbon electricity system.

Several technologies exist or are under development for large-scale energy storage. Pumped-Storage Hydroelectricity (PSH) is the most common one and covers a power range varying from a few hundred of megawatts to a few gigawatts. It accounts for more than 99% of the worldwide bulk storage capacity, representing around 140 GW over 380 locations [1]. Reported roundtrip efficiencies are typically between 70% and 85%. These systems have a low energy density and require the construction of large water reservoirs, leading to a high environmental impact. In addition, the most suitable locations have already been used in developed countries.

At a lower power range varying from a few tens to a few hundreds of megawatts, Compressed-Air Energy Storage (CAES) is at an advanced stage of development but accounts only 2 power plants until now: a 290 MW plant in Huntorf, Germany (1978) [2], and a 110 MW plant in McIntosh, USA (1991) [3]. Reported roundtrip efficiencies are around 50% and the capital cost of CAES power plants is competitive with PSH. Much higher efficiencies up to 70% could be achieved by Advanced Adiabatic CAES (AA-CAES) [3-6] as the second generation technology which is still at an early stage of development. Storage systems such as PSH, CAES and AA-CAES generally require specific sites (especially for large powers).

Among other technologies (Liquid Air Energy storage for example: [7]), thermo-electric energy storage (TEES) is a promising alternative to existing technologies that could provide widespread and large-scale electricity storage. During periods of excess electricity generation, a vapor compression heat pump consumes electricity and transfers heat between a low-temperature heat source and a higher temperature heat sink. The temperature difference between the heat sink and the heat source can be maintained for several hours, until a power cycle is used to generate electricity during peak consumption hours.

Mercangöz et al. [8] showed that the first study on Thermo-Electric Energy Storage date back to the 1920s and described the general concept of this technology, based on two-way conversion of electricity to and from heat. The authors have analyzed a TEES system with CO_2 transcritical cycles, hot water and ice tanks as storage reservoirs. The ABB Corporate Research Center [9-10] described a way to store electricity using two hot water tanks, an ice tank and CO_2 transcritical cycles. For similar systems, Morandin et al. [11-12] calculated a 60% maximum roundtrip efficiency for a base case scenario with turbomachinery efficiencies given by manufacturers.

Sensible heat storage with hot water tanks is often considered, since water has high thermal capacity, cheaply available and environmental-friendly. Latent heat storages based on phase-change materials (PCMs) have also been widely investigated. The heat sink of the system can be either the ambient or ice. This second option ensures a constant low-pressure for the process that is favorable to turbomachines.

CO_2 is a natural refrigerant with many advantages. It is a low-cost fluid that is non-toxic, non-flammable, chemically stable, and cheaply available. In addition, the high fluid density of supercritical CO_2 leads to very compact systems. Many studies have been published to evaluate the potential of supercritical CO_2 as working fluid in power cycles and heat pumps [13-14]. Cayer et al. carried out an analysis [15] and an optimization [16] of CO_2 transcritical cycle with a low-temperature heat source. More recently, the use of CO_2 for multi-megawatt power cycles has reached a commercial step with the American company Echogen [17]. In parallel, underground thermal energy storage appears to be an attractive solution [18].

The purpose of this article is to introduce a new concept of Thermo Electric Energy Storage process for large scale electric applications, based on CO_2 transcritical cycles and ground heat storage. The association of such cycles and ground storage constitutes the originality of the project. The conceptual design of such TEES system is addressed here from thermodynamic and thermofluidic points of view and economic analyses are left for future work.

Section 2 is devoted to thermodynamic cycle considerations. Section 3 deals with ground heat storage description and simulation. Section 4 describes the experimental set-up of heat storage and the first results.

2. Thermodynamic analysis

The investigated thermo-electric energy storage system is a massive storage concept that includes:

i- a hot reservoir made of a set of ground heat exchangers in a low diffusivity rock;
ii- a cold reservoir using either ice;
iii- two thermodynamic cycles as a charging process and a discharging process both using CO_2 as a fluid.

The basic overviews of these two processes are given respectively by Fig. 1. All the components of each process are considered as open systems in steady state. The thermodynamic model is implemented in the Engineering Equation Solver (EES) software [19]. A detailed model has been developed and is extensively described in previous papers [20].

During the off-hours, the charging process consists of a transcritical heat pump cycle characterized by 6 main steps: the working fluid leaves the cold reservoir heat exchanger as a saturated vapour at $T_1 = T_{cold} - \Delta T_{min}$ and is internally superheated (1 → 2) through a regenerator, before being adiabatically compressed (2 → 3) with a mechanical compressor with isentropic efficiency ($\eta_{s,c}$ = 85 %). At the compressor outlet, the fluid at $T_3 = (T_{hot})_{max} + \Delta T_{min}$ and supercritical high pressure P_3 = HP is first cooled through the hot reservoir exchangers (3 → 4) releasing heat to the ground, then subcooled through the regenerator (4 → 5) releasing heat to the first flow. The fluid at a liquid state passes into an expansion valve (5 → 6) to reach the subcritical low pressure and is finally evaporated through the cold reservoir exchanger (6 → 1).

During the peak-hours, the discharging process consists of a transcritical Rankine cycle characterized by 6 main steps: the working fluid leaves the cold reservoir heat exchanger as a saturated liquid at $T_1' = T_{cold} + \Delta T_{min}$ and is adiabatically compressed (1 → 2) in a feed pump with isentropic efficiency ($\eta_{s,p}$ = 80 %). At the outlet of the pump, the fluid at a supercritical high pressure P_2' is first preheated through the regenerator (2 → 3), then heated further through the hot reservoir exchanger (3 → 4) destocking heat from the ground. At the entrance of the turbine, the fluid at a defined temperature $T_4' = (T_{hot})_{max} - \Delta T_{min}$ is adiabatically expanded (4 → 5) to the subcritical low pressure delivering a mechanical work with isentropic efficiency ($\eta_{s,t}$ = 90 %). Finally, the fluid is cooled in the regenerator (5 → 6) before being condensed through the cold reservoir exchanger (6 → 1).

As a preliminary work, pressure losses in the thermodynamic cycles are neglected. Simulation of the ground heat storage system will enable to estimate the head losses in that component and adjust the cycle parameters.

Based on the previous modelling, it is possible to carry out a parameter analysis of the system. It is possible to reach roundtrip efficiencies up to more than 50% with high storage temperatures and ΔT_{min}=1K, on condition that a regenerator is used in both heat-pump and ORC cycles. Detailed results can be found in [20]. In particular a very interesting configuration can be found in Figure 2. The value of ΔT_{min} has been discussed in [20].

We have also investigated the interest of having an architecture with a combination of two-stage turbine configuration of the power system system and a two-phase turbine configuration in the heat-pump system with regenerations. A maximum value of 65% in efficiency could be achieved with such a system.

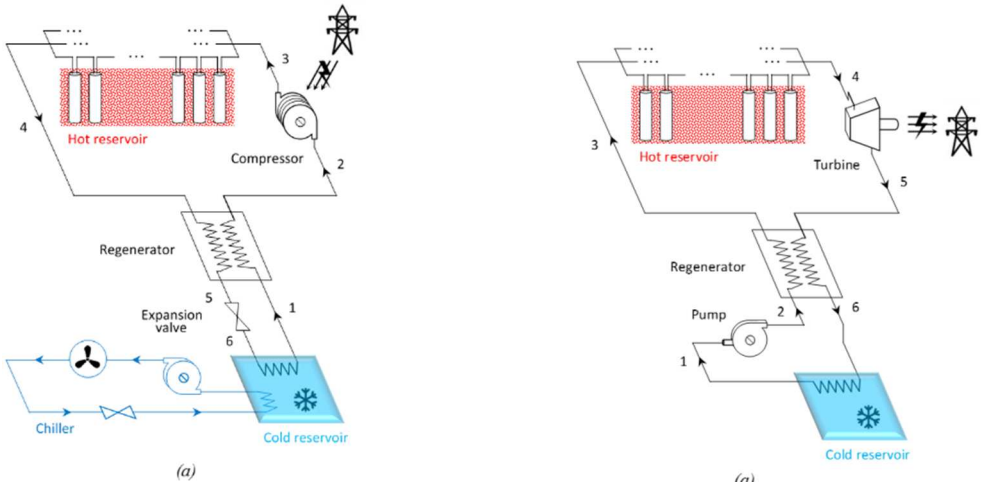

Fig. 1. a) Charging process, b) Discharging process

3. Ground heat storage

3.1. Description and modelling approach

The hot reservoir is made of 2160 identical geothermal exchangers organized in a serial-parallel layout (Figure 3a): there are 48 parallel series of 45 exchangers (radially distributed in the ground). Each exchanger is made of silicone rubber and is composed of a central circular pipe (11.8 cm diameter) used for fluid injection and of an annular return pipe (12.2/20 cm inner/outer diameter) in contact with the surrounding rock as showed in Figure 3b. The distance between adjacent exchangers is 0.5 m. Concerning the fluid flow in the exchangers, please note that the flow direction is from the first (placed at the centre of the storage) to the last exchanger of a series during charge while it is the opposite during discharge: in this way the central exchanger is always the hottest and the peripheral one is the coldest (thus heat losses are minimized).

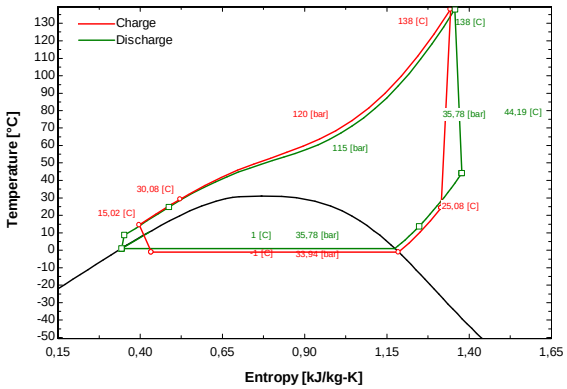

Fig. 2. a) T-S diagram for hot storage at 130°C and cold storage at 0°C

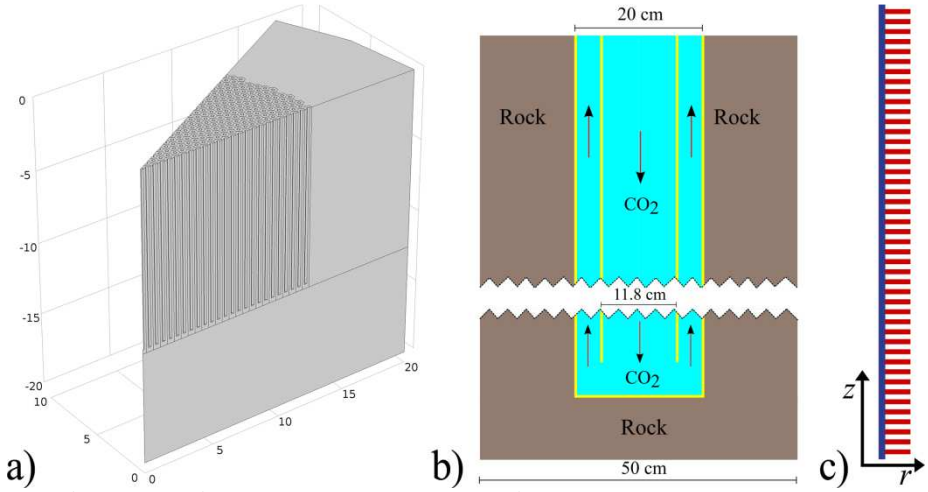

Fig 3. a) Drawing of a 30° sector of the ground heat storage, b) sketch of a single coaxial exchanger, c) 1D/2D computational model (deformed in the radial direction) - fluid domain (blue) and rock domains (red)

The ground heat storage is the central part of this system, but it is also the most complex part to model, therefore several different approaches have been used for the purpose. The main difficulties come from the particularly high Reynolds number (between 10^5 and 10^6) in the exchangers, the large size of the storage and the different time-scales of the process (from seconds, for the flow dynamics, to days, for the heat storage behaviour during multiple charge/discharge cycles). As a consequence, a detailed conjugate heat transfer CFD study was viable only for a single exchanger and for very short durations. However in order to optimize the system we need to model several charge/discharge cycles considering at least a series of 45 exchangers (that is representative of the behaviour of the whole reservoir). Thus, we decided to resort to a 1D model for the thermo-fluid dynamic behaviour of CO_2 inside the exchangers, coupled with a 2D axisymmetric model for the heat transfer inside the rock. In this model the interactions between the exchangers (i.e., heat conduction between the rock surrounding each exchanger) and the heat losses toward the rock surrounding the whole heat storage are assumed to be negligible. The former can be neglected since the temperature difference between adjacent exchangers is small, while the latter are important only during the start-up phase when the temperature of the rock that surrounds the heat storage is different from the temperature of the rock surrounding the peripheral exchangers. Please note that in the one-dimensional thermo-fluid dynamic model both the injection pipe and the annular return in contact with the rock are considered: all the pipes are connected and create a single computational domain for the fluid, aligned with the positive vertical direction (see Figure 3c). Due to the intrinsic unsteadiness of the heat storage system, it is fundamental to adopt an unsteady model for the energy transport (both for fluid and rock). In addition, despite the temporal variation of mass flow rate and pressure is gradual, a transient model has to be used also for the flow dynamics because of the strong coupling between enthalpy, density and velocity.

The 1D/2D model is quite fast and at the same time physically-based however it is not suited for modeling the whole ground heat storage and taking into account both the interactions between exchangers and the heat losses. For this reason an simpler 0D model for the fluid, based on the solution of global mass and energy balances for each exchanger, has been developed. The model is validated by comparison with the 1D model considering the same conditions for the rock (no heat losses and no interactions between exchangers). However this kind of model for the fluid can be easily coupled with any heat conduction model for the rock thus allowing the simulation of the real geometry of the ground heat storage (or a part of it as in the 30° sector model shown in Figure 3a).

3.2. Mathematical models

The governing equation for the heat transfer in the rock is a simple transient heat conduction equation with constant coefficients. A convective heat transfer boundary condition is applied on the boundary in contact with the fluid:

$$-\lambda_R \nabla T_R \cdot \boldsymbol{n} = \Gamma\left(T - T_R\right) \quad (1)$$

where T_R and λ_R are rock temperature and thermal conductivity, respectively. T and Γ are fluid temperature and heat transfer coefficient, respectively and $\boldsymbol{n}$ is the outward pointing normal.

In the 1D model the governing equations (mass, momentum and energy balances) for the fluid are as follows:

$$\frac{\partial \rho}{\partial t} + \frac{1}{A}\frac{\partial\left(\rho U A\right)}{\partial z} = 0 \quad (2)$$

$$\frac{\partial\left(\rho U\right)}{\partial t} + \frac{1}{A}\frac{\partial\left(\rho U U A\right)}{\partial z} = -\frac{\partial p}{\partial z} - \frac{f \rho U \left|U\right|}{2 D_h} \quad (3)$$

$$\frac{\partial\left(\rho h\right)}{\partial t} + \frac{1}{A}\frac{\partial\left(\rho U h A\right)}{\partial z} = q \quad (4)$$

where ρ, U, p and h are respectively density, velocity, pressure and enthalpy of the fluid. q is a volumetric energy source/sink that accounts for the heat transfer from/to the rock surrounding each exchanger, A is the pipe cross-sectional area, f is the Darcy–Weisbach friction factor and D_h is the pipe hydraulic diameter. For simplicity the gravity term in the momentum balance has been neglected since the gravitational pressure drop is small compared to the absolute pressure. Finally, to get a closed set of equations an equation of state for the fluid must be specified; fluid density and temperature are computed as a function of the dependent variables: $\rho = \rho\left(h, p\right)$; $T = T\left(h, p\right)$.

The volumetric heat source/sink of the i^{th} fluid cell q_i is computed dividing the power transferred to/from the fluid from/to the rock by the cell volume V_i:

$$q_i = \frac{\Gamma_i S_i \left(T_{R_b} - T_i\right)}{V_i} \quad (5)$$

where S_i is the area of the face through which the heat transfer takes place and T_{R_b} is the rock temperature at the fluid-rock boundary. Obviously the heat source/sink is equal to zero in the cells belonging to the injection pipe. Please note that the heat transfers between annular and injection pipe have been neglected since the latter is thermally insulated. The reader is referred to [21] for a detailed description of the model.

For each exchanger the 0D model governing equations (mass and energy balance) are:

$$\frac{d\rho}{dt}\forall + \left(G_{out} - G_{in}\right) = 0 \quad (6)$$

$$\frac{d\left(\rho h\right)}{dt}\forall + \left(G_{out} h_{out} - G_{in} h_{in}\right) = Q \quad (7)$$

where $\forall$ is the fluid volume (including the fluid contained in both annular and circular pipe), Q is the power transferred from/to the rock and G is the mass flow rate. As in the 1D model: $\rho = \rho\left(h, p\right)$; $T = T\left(h, p\right)$. Please note that the momentum balance equation simply reduces to a pressure drop equation. This equation has

been neglected since the overall pressure drop is sensibly smaller than the absolute pressure: head losses (distributed and localized) are neglected and the fluid pressure is assumed to be the same for all the exchangers. The total power transferred to/from the fluid is computed integrating the local power over the fluid-rock surface:

$$Q = \int_S \Gamma \left(T_R - T \right) dS \qquad (8)$$

Finally an hypothesis on the outlet enthalpy h_{out} must be introduced. It's effect on the accuracy of the 0D model is very significant. The error will be quite large if we simply assume $h_{out} = h$, while it can be minimized if we compute h_{out} using a quadratic interpolation based on h_{in}, h and the enthalpy of the next exchanger. For each exchanger equations (6) and (7) can be solved explicitly computing G_{out} and h, respectively. Please note that the governing equations are solved sequentially from the first to the last exchanger of a series (following the flow direction), thus properly updating the inlet mass flow rate and enthalpy for each exchanger (set to the outlet values of the previous exchanger).

3.3. Results

Using the models described in the previous section, a preliminary optimization of the ground heat storage is performed. The objective is to increase the exergy efficiency η_{ex}, computed based on the total amount of CO_2 exergy extracted from/sent in the storage:

$$\eta_{ex} = \left(Ex_{out} - Ex_{in} \right)_{\text{discharge}} / \left(Ex_{in} - Ex_{out} \right)_{\text{charge}} \qquad (9)$$

This value gives an estimation of what would be the overall electrical efficiency of the storage system if we had ideal Carnot engines to produce heat (during charge) and electricity (during discharge). Some simulation parameters have been fixed, in particular: number of exchangers in a series (n. 45), CO_2 inlet temperature and outlet pressure during charge (411.15 K and 12 MPa) and discharge (303.15 K and 12 MPa). In the "optimized" configuration we considered: 6h charge with G = 1.75 kg/s and 4h discharge with G = 2.5 kg/s, 30 m long exchangers (note that 18 cycles have been modelled). Some results of this simulation are shown in Figure 4 while the evolution of the exergy efficiency is shown in Figure 5a. The simulations show that the errors introduced using the 0D model are small (<1K), provided that the above mentioned quadratic interpolation is employed for computing h_{out} (see Figure 5b).

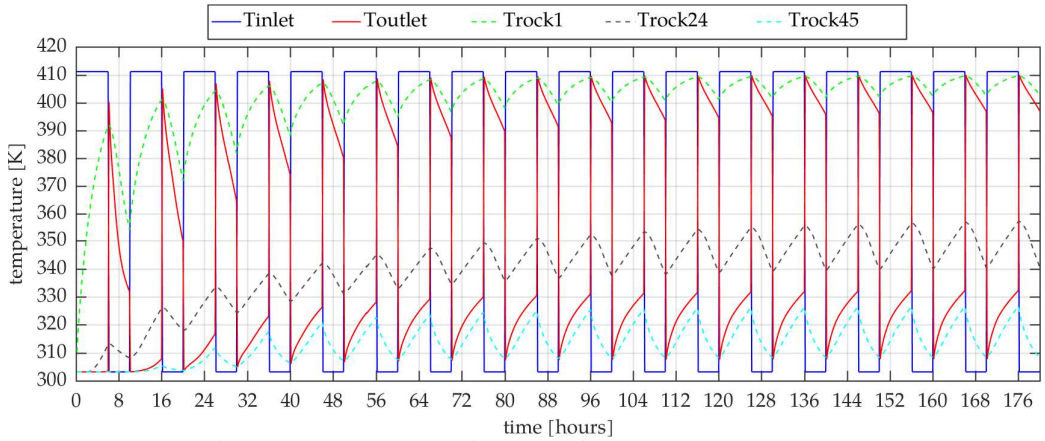

Fig. 4. Temporal evolution of inlet and outlet temperature for a series of exchangers (continuous lines) and volume-averaged rock temperature for 1st, 24th and 45th exchanger (dashed lines)

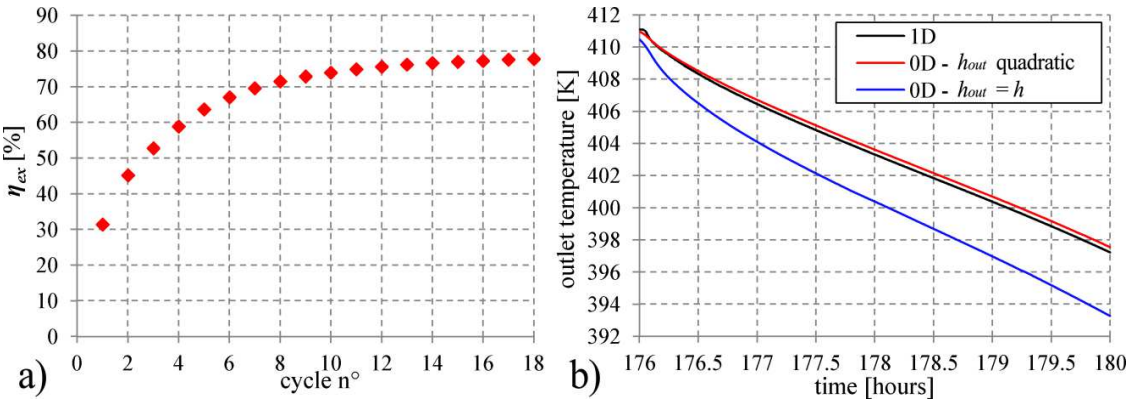

Fig. 5. a) Evolution of the exergy efficiency of the heat storage, b) comparison 0D and 1D model - temporal evolution of outlet temperature during last discharge

4. Experimental set-up

4.1. Description

The experimental test loop constructed for the present study is schematically introduced in Figure 6. Only the main CO_2 circuit is detailed in this picture; for clarity reasons, cold water and hot oil circuits are just mentioned. The main CO_2 circuit is composed of a liquid CO_2 pump, a supercritical heater, the test sections, two absolute pressure transducer, a differential transducer, a pressure regulator, a condenser, a CO_2 tank, a subcooler, a flow meter and various thermocouples.

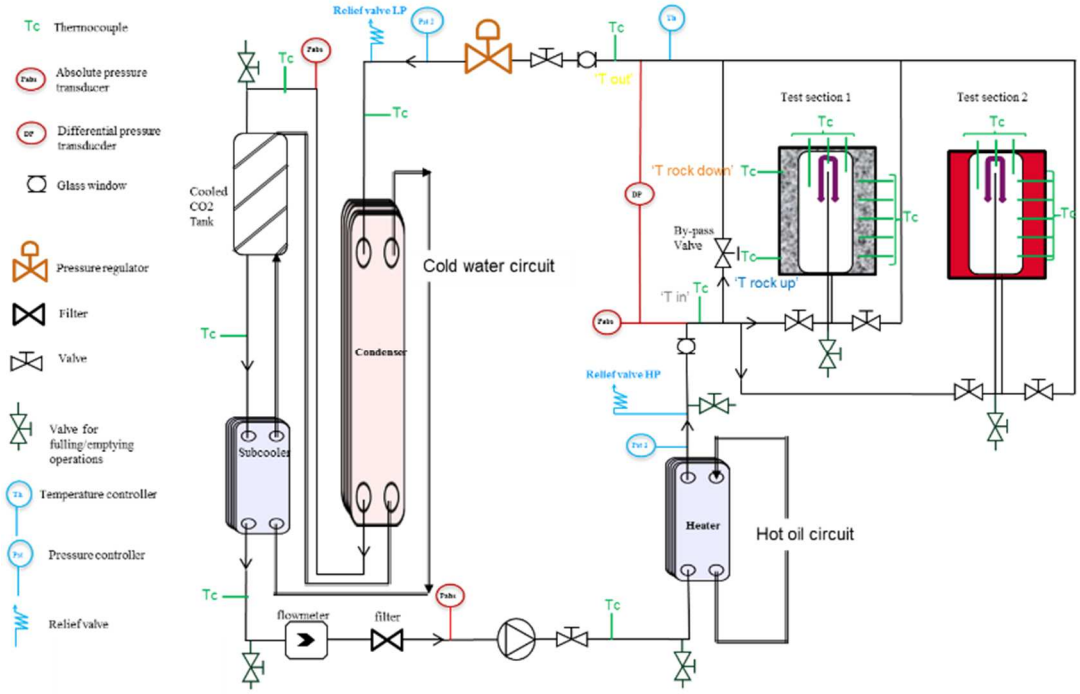

Fig. 6. Schematic draw of CO2 loop

The test loop was filled with CO_2 with purity of 99.5%. Liquid CO_2 is circulated and compressed by a three head diaphragm pump (model LEWA ECOFLOW LDC3) which allows independent controls of discharge pressure and mass flow rate.

The fluid passes through the pre-heater (5 kW hot oil heating exchanger) to adjust the temperature at the inlet of the test section. After entering the expansion valve, the pressure is lower than the critical pressure, and the fluid is condensed (5 kW cold water exchanger), stored in the CO_2 tank (connected to a 2 kW cold water cooling loop) and subcooled (2 kW cold water cooling circuit) to increase its density and its viscosity and to avoid cavitation before circulated by the CO_2 pump.

As illustrated in Figure 6, two test sections can operate in parallel. Each section is a 1.6 m-long vertical heat exchanger (Figure 7) where CO_2 is injected at the top in a 40 mm diameter section. Both test sections have the same geometrical dimensions which approximately correspond to the industrial configuration at a scale of 1:10. The only difference between test sections is that the first is surrounded by granite cylinder that is heated or cooled, whereas the second is heated with a controlled electrical system. This last test section also contains more internal temperature measurements than the first.

The temperature in the loop and in the test section (CO_2, oil, water and granite) were measured using K-type thermocouples calibrated with an accuracy of 0.5 °C. Pressures were measured with an error less than ±0.15%. The mass flow rate of carbon dioxide was measured with an accuracy of 0.1% using a Coriolis mass flow meter.

4.2. First results on charge/discharge behaviour

The objectives of the tests are to experimentally validate the storage concept and to provide experimental data for the validation of the numerical models. Despite both section have been insulated, it seems that the heat losses are not negligible and consequently the temperature differences are larger than in the industrial configuration. In this section we present some results on charge/discharge behaviour. We have investigated experimentally two strategies for charging/discharging process.

4.2.1 Long charge and discharge

The first “natural” strategy is to have a “long” charge and discharge. The evolution of CO_2 temperature in at inlet and outlet of the test section is shown in Figure 8. The inlet condition is rapidly established whereas the outlet has a larger characteristic time. The evolution of rock temperature is also presented: during charge the rock temperature at the bottom of the test section is higher than temperature at the top while it is the opposite during discharge.

Fig. 7. Photographs of CO2 loop and two vertical test sections

When the discharging process begins there is an abrupt change of CO_2 inlet temperature but the rock temperatures continue to increase during the first minutes of the discharging process due to the thermal inertia of the rock. Using inlet and outlet temperatures it is possible, knowing flow rate and pressure, to calculate an instantaneous power balance (Figure 8). Some irregularities can be explained by changes of the flow rate.

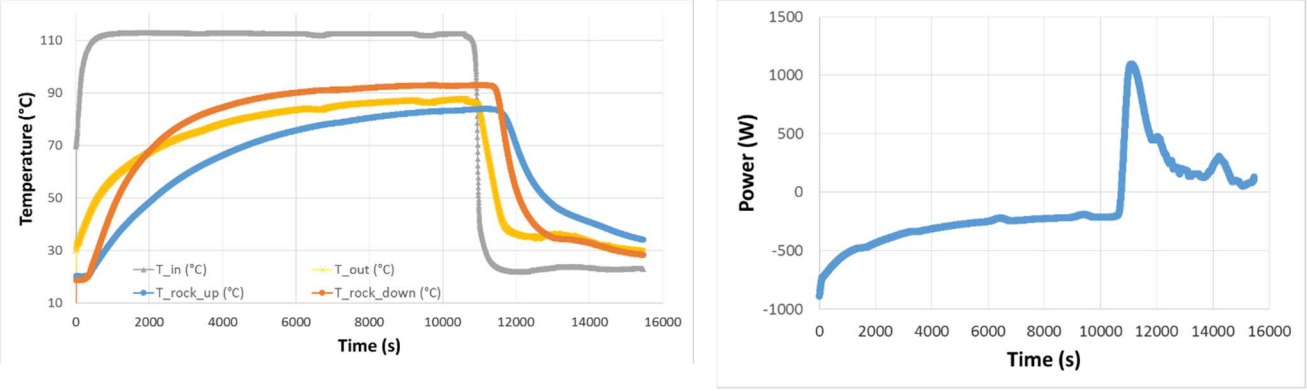

Fig. 8. Evolution of temperature (left) and heat rate (right). Locations of thermocouples are mentioned in Fig. 6.

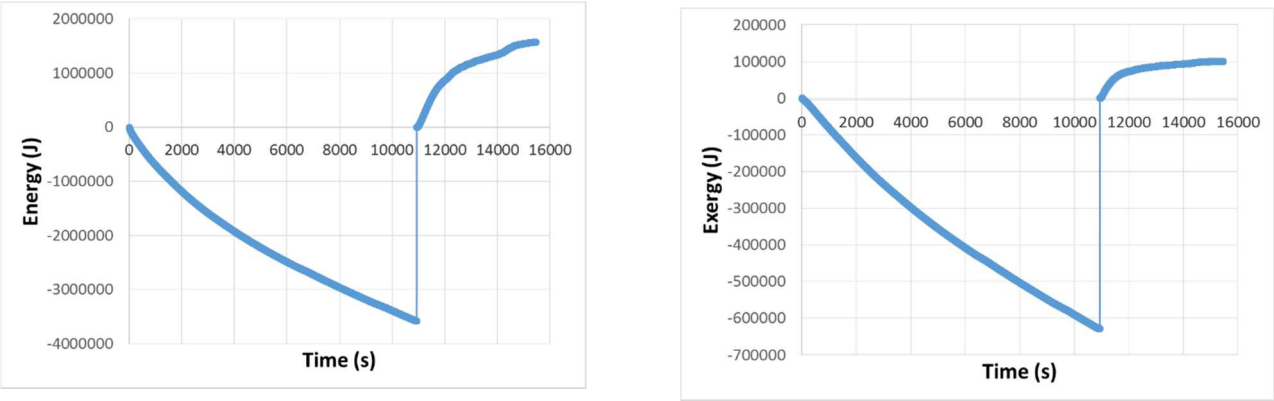

Fig. 9. Evolution of cumulated energy (left) and exergy (right)

Integrating over time we can compute the cumulated energy (Figure 9). A balance between the two processes can be also performed: the cumulated energy differences between charge and discharge can be explained by losses and “too short” recovery time. Regarding exergy, the efficiency is very low (16%). These small values encourage us to investigate another strategy.

4.2.2 Short charge and discharge

The second strategy consists in performing a first long charge and then shorter charge and discharge cycles. A longer discharging process can also occur at the end. The trends of fluid and rock temperatures during the first long charge are similar to the ones described in the previous paragraph. The same qualitative behavior can be seen in the short charge/discharge cycles. We notice that in the first discharging process the temperatures are higher; the next cycles seem to be approximately similar. These trends can be also seen in the instantaneous power balance (Figure 10). Cumulated energy and exergy can be calculated. They show higher recovery values (Figure 11) than in previous section.

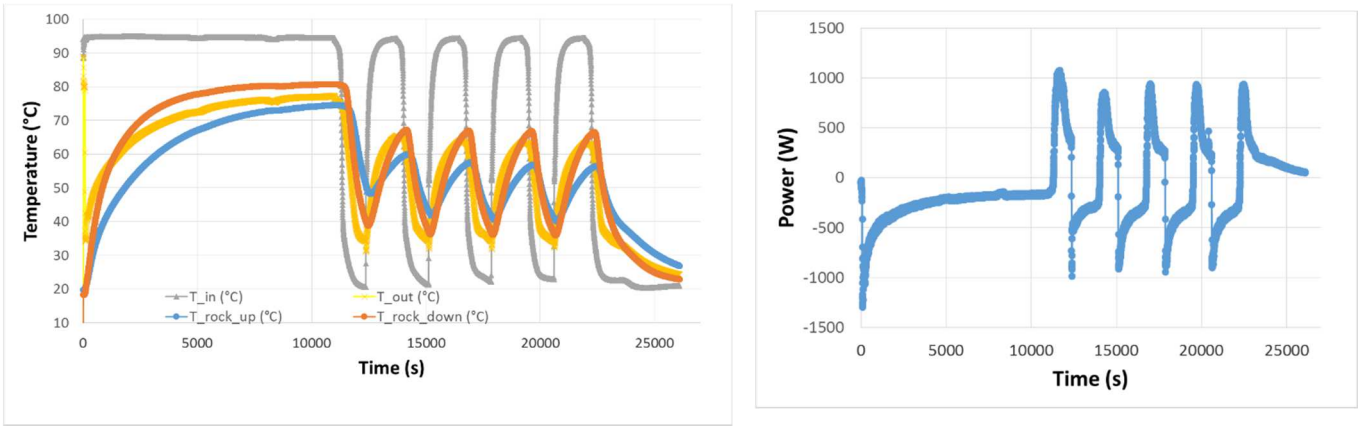

Fig. 10. Evolution of temperature (left) and heat rate (right). Locations of thermocouples are mentioned in Fig. 6.

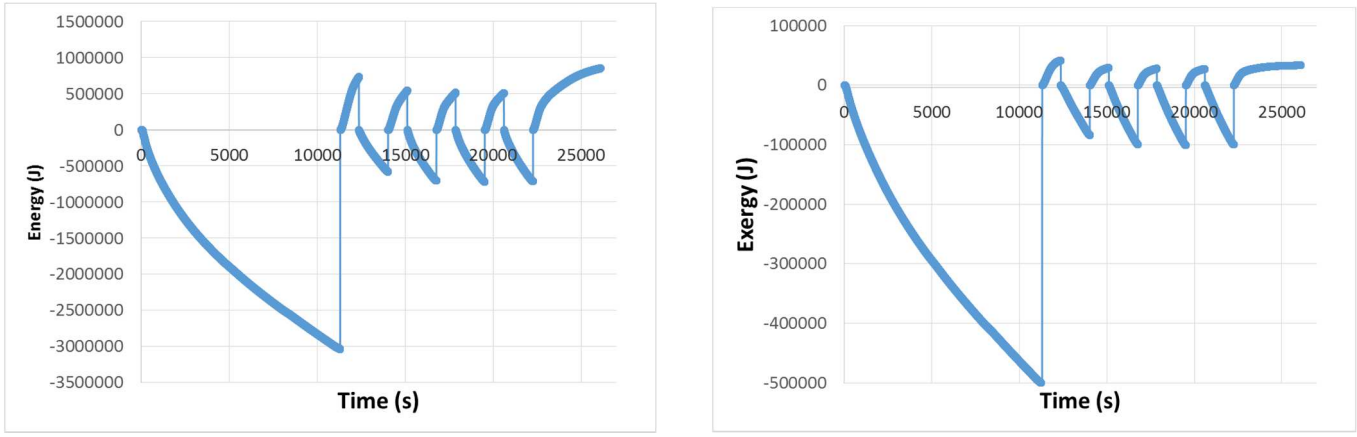

Fig. 11. Evolution of cumulated energy (left) and exergy (right)

5. Conclusion

The aim of this work is to assess the performance of a massive electricity storage involving CO_2 transcritical cycles and using the ground as a heat reservoir and reservoir using ice (or phase-change material) for latent cold storage. The parametric study of the charging and discharging processes has shown roundtrip efficiencies up to

more than 50% given by high storage temperatures with a regenerative systems and 65% with complex expansion processes.

In addition, simulations of flow inside heat exchanger and within geothermal system are performed with different approaches. The first preliminary results show that such numerical tool is able to represent large off-design conditions of the global system. In parallel an experimental work is in progress to provide temperature measurements in the hot storage in order to validate the simulations.

Further work through the SELECO2 project will include turbomachinery, cold storage designs and economic considerations in order to have a more detailed overview of the system. Furthermore further transient simulations of whole storage system will be performed to verify the efficiency values and the general interest of the device.

Acknowledgements

The authors acknowledge the support of Agence Nationale de la Recherche (ANR), under grant ANR-13-SEED-0004 (project SELECO2) and all participants of the project (ENGIE, IMFT, BRGM, CEA, ENERTIME).

References

[1] ENEA Consulting. Facts & Figures : Le Stockage d'Energie. 2012.
[2] Crotogino F, Mohmeyer K-U, and Scharf R. Huntorf CAES: More than 20 Years of Successful Operation. Proc of SMRI Spring Meeting, Orlando, Florida, USA, 15-18 April 2001.
[3] PowerSouth Energy Cooperative. CAES McIntosh Alabama.
[4] "Search Project", 2013. http://www.asprom.com/stockage/hadj.pdf
[5] Chris Bullough, Christoph Gatzen, Christoph Jakiel, Martin Koller, Andreas Nowi, Stefan Zunft, Advanced adiabatic compressed air energy storage for the integration of wind energy, in: Proceedings of the European Wind Energy Conference, London UK, 2004.
[6] Grazzini G, Milazzo A. Thermodynamic analysis of CAES/TES systems for renewable energy plants. Renewable Energy 2008;32:1998–2006.
[7] Giuseppe Leo Guizzi, Michele Manno, Ludovica Maria Tolomei, Ruggero Maria Vitali, Thermodynamic analysis of a liquid air energy storage system, Energy, Volume 93, Part 2, 15 December 2015, Pages 1639-1647
[8] Mercangöz M, Hemrle J, Kaufmann L, Z'Graggen A, Ohler C. Electrothermal energy storage with transcritical CO2 cycles. Energy 2012; 45: 407–415.
[9] Mercangoez M, Hemrle J, Kaufmann L. Thermoelectric energy storage system having two thermal baths and method for storing thermoelectric energy. Patent EP2241737
[10] Ohler C, Mercangoez M. Thermoelectric energy storage system and method for storing thermoelectric energy. Patent EP2182179.
[11] Morandin M, Maréchal F, Mercangöz M, Buchter F. Conceptual design of a thermo-electrical energy storage system based on heat integration of thermodynamic cycles. Energy 2012;45:375–396.
[12] Morandin M, Mercangöz M, Hemrle J, Maréchal F, Favrat D. Thermoeconomic design optimization of a thermo-electric energy storage system based on transcritical CO2 cycles. Energy 2013; 58: 571–587.
[13] Kim YM, Kim CG, Favrat D. Transcritical or supercritical CO2 cycles using both low- and high-temperature heat sources. Energy 2012; 43: 402–415.
[14] Li M, Wang J, Li S, Xurong Wang, He W, Dai Y. Thermo-economic analysis and comparison of a CO2 transcritical power cycle and an organic Rankine cycle. Geothermics 2014; 50: 101–111.
[15] Cayer E, Galanis N, Désilets M, Nesreddine H, Roy P. Analysis of a carbon dioxide transcritical power cycle using a low temperature source. Applied Energy 2009;86:1055–63.
[16] Cayer E, Galanis N, Nesreddine H. Parametric study and optimization of a transcritical power cycle using a low temperature source. Applied Energy 2010;87:1349–1357
[17] Held T. Initial Test Results of a Megawatt-class Supercritical CO2 heat engine. The 4th International Symposium – Supercritical CO2 Power Cycles; 2014 Sept 9-10; Pittsburgh, USA.
[18] Laninia S, Delaleux F, Py X, Olivès R, Nguyen D. Improvement of borehole thermal energy storage design based on experimental and modelling results. Energy and Buildings 2014;77:393–400.
[19] S.A. Klein, Engineering Equation Solver. F-Chart Software, Middleton, WI, 2010.
[20] Fadhel Ayachi, Nicolas Tauveron, Thomas Tartière, Stéphane Colasson, Denis Nguyen, Thermo-Electric Energy Storage involving CO2 transcritical cycles and ground heat storage, Applied Thermal Engineering, Volume 108, 5 September 2016, Pages 1418-1428.
[21] Macchi EG, Colin C, Tartière T, Nguyen D, Tauveron N. Thermoelectric energy storage based on CO2 transcritical cycles: ground heat storage modelling, 1st European Seminar on Supercritical CO2 Power Systems,2016.